PHILOSOPHICAL TRANSACTIONS A

royalsocietypublishing.org/journal/rsta

Research

Cite this article: von Jackowski A, Grosse J, Nöthig E-M, Engel A. 2020 Dynamics of organic matter and bacterial activity in the Fram Strait during summer and autumn. *Phil. Trans. R. Soc. A* **378**: 20190366.
http://dx.doi.org/10.1098/rsta.2019.0366

Accepted: 13 July 2020

One contribution of 18 to a theme issue 'The changing Arctic Ocean: consequences for biological communities, biogeochemical processes and ecosystem functioning'.

Subject Areas:
biogeochemistry, oceanography

Keywords:
Arctic Ocean, seasonality, semi-labile organic carbon, bacteria

Author for correspondence:
Anabel von Jackowski
e-mail: ajackowski@geomar.de

Electronic supplementary material is available online at https://doi.org/10.6084/m9.figshare.c.5069816.

THE ROYAL SOCIETY PUBLISHING

Dynamics of organic matter and bacterial activity in the Fram Strait during summer and autumn

Anabel von Jackowski[1], Julia Grosse[1], Eva-Maria Nöthig[2] and Anja Engel[1]

[1]GEOMAR Helmholz Centre for Ocean Research Kiel, Kiel, Germany
[2]Alfred Wegener Institute, Helmholtz Centre for Polar and Marine Research, Bremerhaven, Germany

AvJ, 0000-0001-6204-5341; JG, 0000-0002-2022-9158; E-MN, 0000-0002-7527-7827; AE, 0000-0002-1042-1955

The Arctic Ocean is considerably affected by the consequences of global warming, including more extreme seasonal fluctuations in the physical environment. So far, little is known about seasonality in Arctic marine ecosystems in particular microbial dynamics and cycling of organic matter. The limited characterization can be partially attributed to logistic difficulties of sampling in the Arctic Ocean beyond the summer season. Here, we investigated the distribution and composition of dissolved organic matter (DOM), gel particles and heterotrophic bacterial activity in the Fram Strait during summer and autumn. Our results revealed that phytoplankton biomass influenced the concentration and composition of semi-labile dissolved organic carbon (DOC), which strongly decreased from summer to autumn. The seasonal decrease in bioavailability of DOM appeared to be the dominant control on bacterial abundance and activity, while no temperature effect was determined. Additionally, there were clear differences in transparent exopolymer particles (TEP) and Coomassie Blue stainable particles (CSP) dynamics. The amount of TEP and CSP decreased from summer to autumn, but CSP was relatively enriched in both seasons. Our study therewith indicates clear seasonal differences in the microbial cycling of organic matter

in the Fram Strait. Our data may help to establish baseline knowledge about seasonal changes in microbial ecosystem dynamics to better assess the impact of environmental change in the warming Arctic Ocean.

This article is part of the theme issue 'The changing Arctic Ocean: consequences for biological communities, biogeochemical processes and ecosystem functioning'.

1. Introduction

Anthropogenic climate change is warming the Arctic Ocean about two to three times faster than the global average [1]. A sensitive indicator of the degree of warming is the loss of sea ice. The year 2018 marked the sixth-lowest sea ice minimum in the nearly 40-year satellite record [2]. Warming of the Arctic results in seasonal, thin and fragile sea ice, thereby completely changing the landscape of icy ecosystems [3–6]. These environmental changes are already influencing phytoplankton dynamics since ice-retreat was responsible for the 30% increase of net primary production between 1998 and 2012 [7]. The change in phytoplankton dynamics could impact bacterial dynamics in the near future since phytoplankton release organic matter that is remineralized by bacteria. This remineralization drives the respiratory flux of CO_2 from the ocean to the atmosphere. Despite the important role of bacteria in the global carbon cycle, the control on heterotrophic bacterial activity in the Arctic is not well-understood.

Recent studies have identified the lability of dissolved organic carbon (DOC) as a major factor controlling bacterial activity in polar environments [8–10]. The lability of DOC can be classified as a continuum from very labile to ultra-refractory DOC: labile components are used within hours to days, while refractory components have a residence time of centuries to millennia. Semi-labile DOC has a turnover of weeks to months, which allows it to accumulate in the upper water column during the productive season [11]. Dominant biochemical components within the semi-labile fraction include dissolved combined carbohydrates (dCCHO) and dissolved hydrolysable amino acids (dHAA) [12–14]. Furthermore, the semi-labile fraction can partition into gel particles, constituting a dynamic continuum from dissolved precursors to single colloids (approx. 1 nm) and macro gels (greater than 1 mm) [15–17]. Polysaccharide-containing micro gels, referred to as transparent exopolymer particles (TEP), are among the best-described micro gels in the ocean. The amount of TEP released into the ocean increases during the senescent bloom phase when phytoplankton growth approaches nutrient depletion [18–22]. Another type of micro gel are Coomassie Blue stainable particles (CSP). CSP are presumably formed by extracellular proteins, but few endeavours have explored their production [23,24]. The organic content that has aggregated as TEP and CSP can serve as substrates for particle-attached bacteria and also provide an important vector for export to the deep sea [25,26].

The degree to which microbial cycling of organic matter is subject to change under the pressure of global warming is difficult to predict. Satellite-based models have the advantage of using annual data and accounting for seasonal dynamics [7,27], but ecosystem or nutrient models rely on *in situ* data, like Forest *et al.* [28]. However, most *in situ* data in the Arctic are collected during the summer. This seasonal data bias is owing to the logistical difficulties of sampling in the Arctic during the dark and colder seasons. The predictions are further implicated by a regional bias since the majority of data for heterotrophic microbial processes are collected in the Beaufort Sea and Chukchi Sea [29]. Our study aimed at filling seasonal gaps by investigating DOM dynamics and bacterial activity in the Fram Strait during summer and autumn. The objective of this study was to assess (i) the seasonal shifts in DOC availability and in BP and (ii) to evaluate seasonal changes in DOM–microbe interactions for carbon-cycling within the pelagic Arctic ecosystem.

2. Methods

(a) Study site

Samples were collected in the Fram Strait with the RV *Polarstern* cruise PS114 from 16 to 23 July 2018 during summer and with the RV *Maria S. Merian* cruise MSM77 from 16 September to 4 October 2018 during autumn (figure 1; electronic supplementary material, table S1). The sampling campaigns were part of yearly measurements in proximity to the Long-Term Ecological Research (LTER) observatory HAUSGARTEN situated in the eastern Fram Strait. The Fram Strait is the only deep gateway to the central Arctic Ocean and is characterized by two distinct hydrographic regimes. In the east, the northward-flowing West Spitsbergen Current (WSC) transports warm saline Atlantic water (AW; $> 2^{\circ}$C; > 34.9 PSU) into the Arctic basin. On the opposite side of the 450 km wide Strait, the southward-flowing East Greenland Current (EGC) transports cold polar water (PW; $< 0^{\circ}$C; < 34.7 PSU) along the Greenland shelf. Here, water masses that were not distinctly characterized as AW or PW were defined as intermediate water (IW).

(b) Discrete sampling parameters

Sampling procedures were identical during both cruises. Seawater samples were collected at five depths (surface; above, in, and below the deep chlorophyll maximum (DCM); 100 m) using a SEA-BIRD CTD rosette sampling system equipped with 24 Niskin bottles. The chlorophyll maximum was identified by running a fluorescence probe on the downward cast of the CTD.

Samples for chlorophyll-*a* were collected on 25 mm GF/F (Whatman, GE Healthcare Life Sciences, UK) and subsequently frozen (-20°C) until extraction using 90% acetone for photometric analyses (Turner Designs, USA), slightly modified after Evans *et al.* [30]. Chlorophyll-*a* was used as a proxy for phytoplankton biomass. Duplicate samples for dissolved organic carbon (DOC) and total dissolved nitrogen (TDN) were filtered through 0.45 µm GMF GD/X filters (Whatman, GE Healthcare Life Sciences, UK) and collected in combusted glass ampoules (8 h, 450°C). DOC/TDN was acidified and stored at 4°C until simultaneous analysis after Engel & Galgani [31] with a detection limit (DL) of 1 mol l^{-1}. Duplicate samples for total dissolved phosphorus (TDP) were filtered through 0.45 µm Acrodisk filters (GHP membrane, Pall Corporation, USA) and frozen (-20°C) until analysis. TDP and dissolved inorganic phosphorus (DIP) were analysed after Murphy & Riley [32] with a DL of 2 µmol l^{-1}. DIP was subtracted from TDP to obtain dissolved organic phosphorus (DOP). Duplicate samples for high-molecular-weight (greater than 1 kDa) dissolved combined carbohydrates (dCCHO) were filtered through 0.45 µm Acrodisk filters, collected in combusted glass vials (8 h, 450°C) and frozen (-20°C) until analysis after Engel & Händel [33] with a DL of 10 nmol l^{-1}. The analysis classified 11 monomers: arabinose, fucose, galactose, galactosamine, galacturonic acid, glucosamine, glucose, glucuronic acid, rhamnose, co-elute mannose and xylose. Duplicate samples for dissolved hydrolysable amino acids (dHAA) were filtered through 0.45 µm Acrodisk filters, collected in combusted glass vials (8 h, 450°C) and frozen (-20°C) until analysis. dHAA were measured with ortho-phthaldialdehyde derivatization by high-performance liquid chromatography (HPLC) [34,35]. The HPLC (Agilent Technologies, USA) was equipped with a C18 column (Phenomenex, USA) with a precision of less than 5% and DL of 2 nmol l^{-1}. The analysis classified 13 monomers: alanine, arginine, aspartic acid, isoleucine, glutamic acid, glycine, leucine, phenylalanine, serine, threonine, tyrosine, valine; and γ-aminobutyric acid (GABA).

Duplicate samples for gel particle analysis were filtered onto 25 mm 0.4 µm-pore sized Nucleopore track-etched polycarbonate filters (Whatman, GE Healthcare Life Sciences, UK). Filters for transparent exopolymer particle (TEP) analysis were stained using Alcian Blue [36] for 5 s, whereas those for Coomassie Blue stainable particles (CSP) were stained with Coomassie Blue [23] for 30 s. Filters were subsequently placed on CytoClear slides (Poretics Inc., USA) and then frozen (-20°C) until analysis. Slides were imaged using an Axioscope A.1 with an attached AxioCam MRC (Zeiss, Germany) at 20× magnification and processed with ImageJ [22]. The image

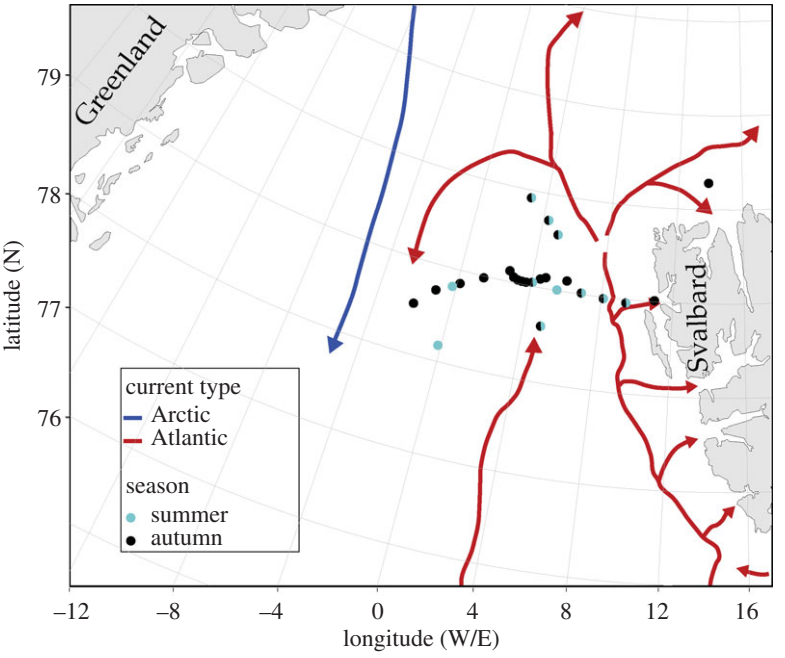

Figure 1. Map of stations within the Fram Strait in the proximity of the LTER observatory HAUSGARTEN. The samples during summer were collected with the RV *Polarstern* on board cruise PS114 from 16 July to 23 July 2018 and during autumn with the RV *Maria S. Merian* on board MSM77 from 16 September to 4 October 2018. Warm-water with Atlantic-origin (red arrows/northward) enters via the West Spitsbergen Current (WSC) in the eastern Fram Strait and cold polar water of Arctic-origin (blue arrows/southward) exits via East Greenland Current (EGC) in the west of the Fram Strait. (Online version in colour.)

processing allowed the determination of particle abundance as well as particle size (area). Particle abundance is of interest for aggregation and degradation processes [37], whereas the size is a measure for estimating the carbon and nitrogen content of the individual gels [38,39].

Samples for cell abundance were fixed with glutardialdehyde (GDA, 25%), and subsequently frozen (−80°C) until further analysis. Prior to analysis, the flow cytometer (FACSCalibur, Becton Dickinson, USA) was calibrated and standardized with TruCount beads (Becton Dickinson, USA). The cells were stained using SybrGreen I (Thermo Fisher Scientific, USA) and subsequently counted by flow cytometry using the Cell Quest 3.3 software with a DL of 2000 events per second. Additionally, subpopulations of low nucleic acid content (LNA) and high nucleic acid content (HNA) bacteria were derived by distinguishing between differences in fluorescence intensity [40–42].

Bacterial production (BP) was measured onboard the research vessels using the microcentrifuge method [43]. Duplicate samples and one killed control (1.5 ml each) were labelled using ^{3}H-leucine (BioTrend, USA) at a final concentration of 20 nmol l^{-1}. ^{3}H-leucine had a specific activity of 100Ci mmol^{-1}. The samples were incubated for 6 h in the dark at 4°C and terminated using trichloroacetic acid (TCA) at a final concentration of 5%. Leucine incorporation was converted into BP by applying a factor of 1.5 kg C mol leucine^{-1} assuming no intracellular isotope dilution [44,45].

(c) Calculations and statistical analysis

In the text and tables, n refers to the number of observations and n_{st} to the number of integrated stations. Stations were integrated over the upper 100 m using trapezoidal integration. The calculations for the carbon and nitrogen content of dCCHO and dHAA were based on carbon

and nitrogen atoms contained in the identified monomers. Carbon content of dCCHO and dHAA was normalized to DOC as % DOC. The incorporation of semi-labile DOC into BP per day (% SL-DOC d^{-1}) was calculated by BP (mmol C m^{-2} d^{-1}) ÷ semi-labile DOC (mmol m^{-2}) × 100.

Statistical analyses were conducted using the software R (v3.5.1) in Rstudio (v1.1.414; [46]). Variables were fed into a statistical mixed model [47,48] including season ('Summer','Autumn') and either depth ('surface', 'above DCM', 'DCM', 'below DCM', '100 m') or water mass ('AW', 'IW', 'PW') as well as their interaction term as fixed factors. The station was regarded as a random factor and the residuals were assumed to be normally distributed and to be homo/heteroscedastic with respect to the different levels. Based on this model, a pseudo-r^2 [49] and an analysis of variances (ANOVA) was conducted, followed by multiple contrast tests (MCT) in order to compare the several levels of the influence factors, respectively. Statistical results are reported in electronic supplementary material, table S2.

Packages used in the scope of this study included PlotSvalbard (v0.7.11, [50]), ggplot2 (v3.2.0, [51]), nlme (v.3.1-139 [52]), piecewiseSEM (v2.0.2 [53]), multcomp (v1.4-10 [54]), lsmeans (v2.30-0 [55]), car(v3.0-2 [56]), FactorMineR (v1.41 [57]) and corrgram (v1.13 [58]).

3. Results

The study area was predominantly ice-free during both summer and autumn. Ice floes were observed north of 79.5°N and west of 0°W/E in summer and north of 79.5°N and further west at 2°W in autumn. Single ice floes were encountered at 'N4' in summer and 'D4' in autumn (electronic supplementary material, table S1). Water temperature ranged from 0.75°C to 6.2°C in summer ($n = 53$) and from 0.52°C to 7.1°C in autumn ($n = 110$; table 1), therefore only characterizing as AT and IW. During both cruises, a fluorescence peak was observed between 20 and 40 m water depth indicating a DCM. However, the fluorescence peak was of lower intensity and occasionally below the detection limit at some stations in autumn. Chlorophyll-*a* ranged from 21 to 209 mg m^{-2} in summer ($n_{st} = 11$) and from 15 to 41 mg m^{-2} in autumn ($n_{st} = 22$) and thus was three times higher in summer compared to autumn (figure 2, table 1). Chlorophyll-*a* concentrations were significantly different in the AW between the summer and autumn (ANOVA $F_{1,136} = 39.4$, $p < 0.0001$; MCT $p < 0.001$; electronic supplementary material, table S2), while concentrations did not significantly change in IW.

(a) Composition of organic matter

DOC ranged from 6029 to 8171 mmol m^{-2} in summer ($n_{st} = 11$) and from 5953 to 8103 mmol m^{-2} in autumn ($n_{st} = 22$). DOC concentrations (table 1) showed no significant seasonal difference (*Mann–Whitney*-test, $p = 0.8$; electronic supplementary material, table S2). Semi-labile DOC made up 8.4 ± 4.7% of total DOC (% DOC) in summer (n=53) and 3.5 ± 0.8% DOC in autumn (n = 110, figures 2 and 4). Semi-labile DOC, and components thereof, significantly correlated with chlorophyll-*a* concentrations (figure 3). Furthermore, semi-labile DOC was significantly different between AW and IW in summer, but not autumn (ANOVA $F_{1,130} = 6.1$, $p < 0.05$; MCT $p < 0.001$; electronic supplementary material, table S2). TDN ranged from 819 to 1287 mmol m^{-2} in summer ($n_{st} = 11$) and from 780 to 1597 mmol m^{-2} in autumn ($n_{st} = 22$). TDP ranged from 31 to 49 mmol m^{-2} in summer ($n_{st} = 11$) and from 38 to 121 mmol m^{-2} in autumn ($n_{st} = 22$). DOP ranged from 5 to 21 mmol m^{-2} in summer ($n_{st} = 11$) and from 2 to 11 mmol m^{-2} in autumn ($n_{st} = 9$).

dCCHO ranged from 43 to 107 mmol m^{-2} in summer ($n_{st} = 11$) and from 24 to 42 mmol m^{-2} in autumn ($n_{st} = 22$). The molecular composition shows that dCCHO was dominated by glucose (14–66 mol%) and co-elute mannose/xylose (14–55 mol%) during both seasons. To investigate a potential change in dCCHO composition along with the quantitative decrease from summer to autumn, we applied principal component analysis (PCA). The first principal component (PC1) explained 51.9% and was primarily influenced by the season (electronic supplementary material, figure S1). The second principal component (PC2) explained 17.7% and was primarily influenced

Table 1. Arithmetic means and one standard deviation of variables determined in the Fram Strait during summer and autumn. The '*n*' refers to the number of observations.

		summer	*n*	autumn	*n*
temperature	°C	4.50 ± 1.49	53	4.59 ± 1.52	110
salinity	PSU	34.84 ± 0.40	53	34.82 ± 0.29	110
chlorophyll-*a*	$\mu g\ l^{-1}$	1.11 ± 1.02	53	0.36 ± 0.29	110
DOC	$\mu mol\ l^{-1}$	73.65 ± 9.04	53	72.46 ± 5.64	110
semi-labile DOC	$\mu mol\ l^{-1}$	6.24 ± 3.49	53	2.52 ± 0.60	104
semi-labile DOC	% DOC	8.4 ± 4.7	53	3.5 ± 0.8	104
dCCHO	$\mu mol\ C\ l^{-1}$	4.65 ± 2.68	53	1.87 ± 0.47	110
dCCHO	% DOC	6.3 ± 3.6	53	2.6 ± 0.7	110
dHAA	$\mu mol\ C\ l^{-1}$	1.59 ± 0.93	53	0.66 ± 0.20	104
dHAA	% DOC	2.1 ± 1.2	53	1.0 ± 0.3	104
semi-labile C : N	ratio	10.7 ± 2.0	53	9.3 ± 1.5	104
TEP particles	$\times 10^6\ l^{-1}$	11.58 ± 8.17	53	7.01 ± 4.80	95
TEP area	$cm^2\ l^{-1}$	1.08 ± 0.71	53	0.42 ± 0.29	95
TEP	$\mu g\ C\ l^{-1}$	21.4 ± 14.5	53	7.1 ± 5.2	95
CSP particles	$\times 10^6\ l^{-1}$	14.64 ± 9.38	53	11.69 ± 7.92	95
CSP area	$cm^2\ l^{-1}$	1.43 ± 1.16	53	1.06 ± 0.74	95
bacterial abundance	$\times 10^5\ ml^{-1}$	9.35 ± 4.36	53	6.41 ± 2.65	110
HNA	%	60.2 ± 7.8	53	50.7 ± 5.5	110
BP	$\mu g\ C\ l^{-1}\ d^{-1}$	0.65 ± 0.47	52	0.14 ± 0.11	110
BP_{cell}	$fg\ C\ cell^{-1}\ d^{-1}$	0.71 ± 0.43	52	0.21 ± 0.11	110

by the depth (electronic supplementary material, figure S1). dCCHO was significantly different between summer and autumn (*Mann–Whitney*-test, $p < 0.0001$) in all depths (ANOVA $F_{4,130} = 17.4$, $p < 0.0001$; MCT $p < 0.01$; electronic supplementary material, table S2). dCCHO contributed 6.3 ± 3.6% DOC to semi-labile DOC in summer (n=53) and 2.6 ± 0.7% DOC in autumn ($n = 110$, table 1).

dHAA ranged from 22 to 62 $mmol\ m^{-2}$ in summer ($n_{st} = 11$) and from 13 to 20 $mmol\ m^{-2}$ in autumn ($n_{st} = 19$). The molecular composition showed that dHAA was dominated by glycine in summer (13–35 mol%; 23.6 ± 4.8 mol%; $n = 53$) and autumn (23–38 mol%; 30.8 ± 2.8 mol%; n=104). The second most abundant dHAA was glutamic acid, which was higher in summer (8–24 mol%; 15.1 ± 3.7 mol%; $n = 53$) than in autumn (7–17 mol%; 10.5 ± 1.7 mol%; $n = 104$). Again, we applied PCA using the relative composition to determine a change in quality and degradation state [59]. PC1 explained 40.1% and was primarily influenced by the depth (electronic supplementary material, figure S2). PC2 explained 12.3% and was primarily influenced by the season (electronic supplementary material, figure S2). There was a significant difference between summer and autumn (*Mann–Whitney*-test, $p < 0.0001$) by depth and water masses (electronic supplementary material, table S2). dHAA contributed 2.1 ± 1.2% DOC in summer ($n = 53$) and 1.0 ± 0.3% DOC in autumn ($n = 104$, table 1).

TEP abundance ranged from 365 to 1936 × $10^6\ m^{-2}$ in summer ($n_{st} = 11$) and from 220 to 1398 × $10^6\ m^{-2}$ in autumn ($n_{st} = 18$). The total area of TEP ranged from 45 to 295 × $10^6\ cm^2\ m^{-2}$ in summer ($n_{st} = 11$) and from 4 to 12 × $10^4\ cm^2\ m^{-2}$ in autumn ($n_{st} = 19$). The area of TEP was significantly different between summer and autumn (*Mann–Whitney*-test; $p < 0.0001$; electronic

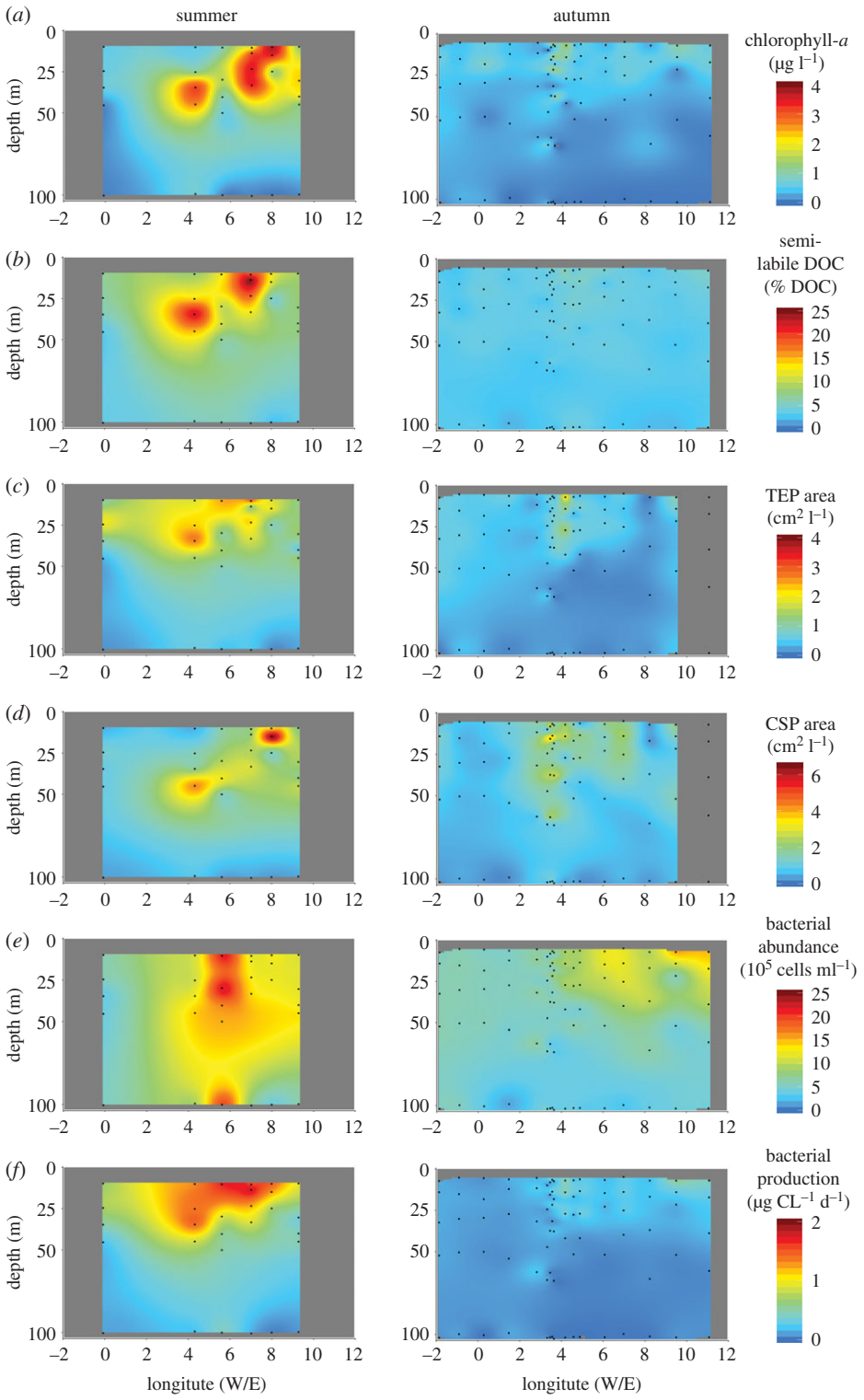

Figure 2. Spatial variability along the approximately 79°N latitude in the Fram Strait during the summer (left) and autumn (right) of 2018. The parameters shown include (*a*) chlorophyll-*a*, (*b*) semi-labile carbon, area of (*c*) TEP and (*d*) CSP, (*e*) bacterial abundance and (*f*) bacterial production (BP). No data are available for the grey shaded region; stations not shown include: N3-N5, NSB1, S3, R1 (electronic supplementary material, table S1). (Online version in colour.)

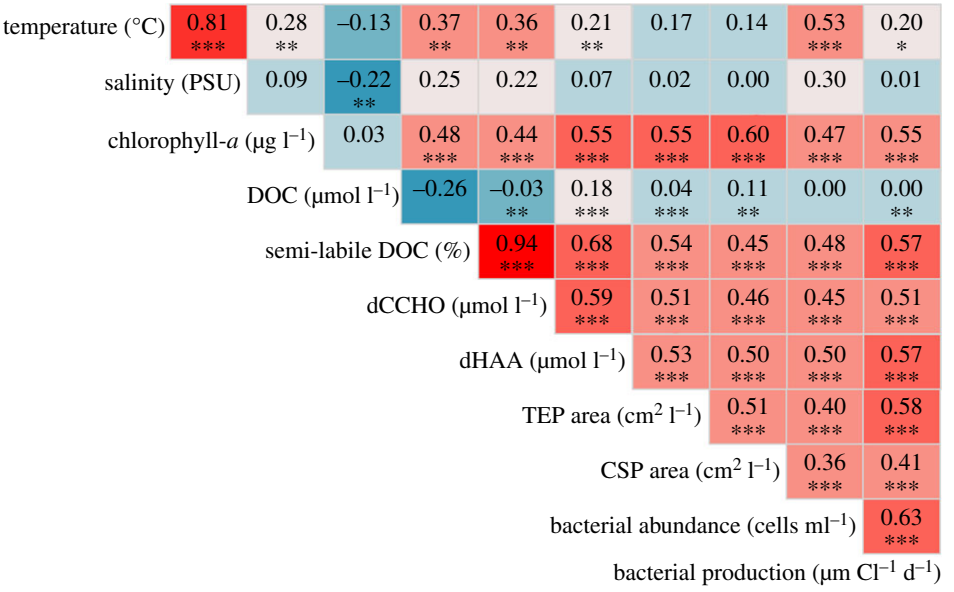

Figure 3. Correlations of physical and biochemical parameters in the upper 100 m of the Fram Strait in 2018. Low correlations are shown in a blue shade, followed by teal, grey, salmon and red indicating a strong correlation. Significances are shown by asterisks as '***' < 0.001, '**' < 0.01, '*' < 0.05 and ' ' > 0.05. (Online version in colour.)

supplementary material, table S2) with the strongest differences in the surface to below DCM (ANOVA $F_{4,118} = 16.0$, $p < 0.0001$; MCT $p < 0.0001$; electronic supplementary material, table S2). Concentration of carbon in TEP (TEP-C) ranged from 82 to 255 mmol m^{-2} in summer ($n_{st} = 11$) and to 19 to 115 mmol m^{-2} in autumn ($n_{st} = 19$). TEP-C relative to the DOC pool was $2.1 \pm 0.9\%$ DOC ($n_{st} = 11$) in summer and $0.7 \pm 0.3\%$ DOC in autumn ($n_{st} = 19$; figure 4). CSP abundance ranged from 672 to 1801×10^6 m^{-2} in summer ($n_{st} = 11$) and from 284 to 2344×10^6 m^{-2} in autumn ($n_{st} = 19$). The total area of CSP ranged from 63 to 377×10^6 cm^2 m^{-2} in summer ($n_{st} = 11$) and from 3 to 25×10^4 cm^2 m^{-2} in autumn ($n_{st} = 19$). The [TEP] : [CSP] ratio (area : area) was 1 : 1.6 in summer and 1 : 3.0 in autumn, reflecting the relative increase of CSP in autumn.

(b) Bacterial distribution and production

Bacterial abundance ranged from 3 to 22×10^5 cells ml^{-1} in summer ($n = 53$) and from 2 to 15×10^5 cells ml^{-1} in autumn ($n = 110$, figure 2). Bacterial abundance was significantly different in AW, but not IW between summer and autumn showing that bacteria behave differently in the two water masses (ANOVA $F_{1,136} = 10.6$ $p < 0.001$; MCT; electronic supplementary material, table S2). Bacterial abundances in AW decreased from $10.34 \pm 4.32 \times 10^5$ cells ml^{-1} in summer ($n = 41$) to $6.02 \pm 2.53 \times 10^5$ cells ml^{-1} in autumn ($n = 59$), compared to the IW where it increased from $5.97 \pm 2.40 \times 10^5$ cells ml^{-1} in summer ($n = 11$) to $6.87 \pm 2.73 \times 10^5$ cells ml^{-1} in autumn ($n = 51$). Yet, the significant correlations with chlorophyll-*a* ($r^2 = 0.47$, $p < 0.001$) and semi-labile DOC ($r^2 = 0.48$, $p < 0.001$, figure 3), indicate that semi-labile DOC controlled bacterial abundances in all water masses. In addition, we differentiated between LNA and HNA. Abundance of LNA ranged from 1 to 9×10^5 cells ml^{-1} in summer ($n = 53$) and 1 to 8×10^5 cells ml^{-1} in autumn ($n = 110$). The abundance of HNA ranged from 2 to 13×10^5 cells ml^{-1} in summer ($n = 53$) and 1 to 9×10^5 cells ml^{-1} in autumn ($n = 110$). Therefore, the fraction of HNA decreased from summer to autumn (figure 4, table 1). The ratio of [HNA] : [LNA] (abundance : abundance) was 1.6 : 1 in summer ($n = 53$) and 1.1 : 1 in autumn ($n = 110$).

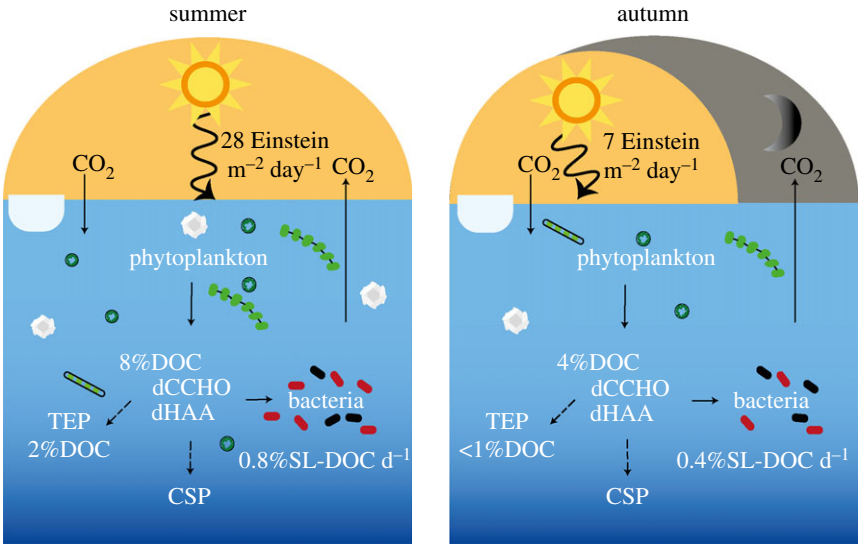

Figure 4. Partitioning of organic carbon between the dissolved and microbial pools for integrated water column of the Fram Strait during summer (left) and autumn (right). Phytoplankton release semi-labile DOM components like dCCHO and dHAA that can further partition into TEP and CSP. The decline in semi-labile DOC triggers a decrease in bacterial incorporation of semi-labile DOC (%SL-DOC d^{-1}) and the bacterial community composition from summer to autumn. HNA bacteria are coloured in red and LNA bacteria in black. PAR data are a monthly estimate from MODIS-Aqua satellite of a 4-km spatial resolution between 1–31 July 2018 for summer and 1–30 September 2018 within 78–80°N and —2°W–13°E from https://giovanni.gsfc.nasa.gov. (Online version in colour.)

BP was measured at 4°C for all samples and ranged from 15 to 75 mg C m^{-2} d^{-1} in summer ($n_{st} = 11$) and from 3 to 15 mg C m^{-2} d^{-1} in autumn ($n_{st} = 22$). BP was more than four times higher in summer than in autumn (table 1) and significantly changed in all depths (ANOVA $F_{4,129} = 16.9$ $p < 0.001$; electronic supplementary material, table S2). Again, the significant correlation to chlorophyll-*a* as well as labile components (figure 3) suggests that the lability was responsible for the significant difference in BP between summer and autumn. Carbon incorporated into BP was 0.80 ± 0.37% SL-DOC d^{-1} in summer ($n = 11$) and 0.45 ± 0.27% SL-DOC d^{-1} in autumn (n=22; figure 4).

4. Discussion

Our study focuses on potential changes in DOM composition and the dependency of microbial activity in the Fram Strait between summer and autumn. Conditions during the field sampling in summer reflected the late-bloom phase of the main annual phytoplankton bloom development, which typically occurs in June/July [60]. Phytoplankton release an increased amount of bioavailable DOM towards the end of the bloom [33,61], which can explain the observed twofold higher concentration of dCCHO and dHAA in summer compared to autumn. The observed concentrations of 0.80 ± 0.46 µmol dCCHO l^{-1} in the Fram Strait are close to the 0.90 ± 0.32 µmol dCCHO l^{-1} reported for the Beaufort Sea during summer [62]. Accordingly, the average contribution of dCCHO to the DOC pool (% DOC) of 6.3 ± 3.6% DOC is lower than the 8 ± 3% DOC in Beaufort Basin [62]. In addition to the spatial variations, carbohydrates displayed a temporal variation. To the best of our knowledge, this is the first study showing a twofold decline of dCCHO between summer and autumn for the Arctic. The observed change is similar to the decline from approximately 4% DOC in summer to approximately 2% DOC in winter shown for the euphotic zone of the Sargasso Sea [13]. Furthermore, the decrease by 3.7%

DOC until autumn resembles the trend between the upper 80 m and the deep Beaufort basin in summer (3% DOC [62]). This indicates that the seasonal production of bioavailable DOM within the Fram Strait was almost degraded until autumn. The remaining carbohydrates in the water column exhibited a more refractory state but could be a potential substrate for bacteria during the winter. Although carbohydrates are an important carbon and energy source for bacteria, amino acids also serve as a nitrogen source and directly support biomass production [63–69]. The seasonal trajectory of dHAA appears to increase from 1.5% DOC in spring [64] to 2.1–2.3% DOC in summer ([64], this study) and subsequently decreases to 1.0 ± 0.3% DOC until autumn. In particular, the drawdown of dHAA below the 1.1% DOC, a threshold set for the least reactive fraction of semi-labile DOM using bioassay experiments [65], indicates that the labile dHAA reservoir is likely to be exhausted in autumn. Changes in the seasonal dHAA reservoir are furthermore apparent in the amino acid composition (electronic supplementary material, figure S2). For example, the molar fraction of glutamic acid increased by 4.7 mol% between spring and summer [64], whereas it decreased by 4.6 mol% between summer and autumn in this study. In contrast, glycine decreased between spring and summer by 2.3 mol% [64], while it increased between summer and autumn by 7.5 mol% in this study. Consequently, the amino acid reservoir appears to be highly dynamic throughout the year with an increase of semi-labile components toward summer and a rapid utilization until autumn.

BP persists in different magnitudes throughout all seasons in the Arctic, albeit with a strong decrease from the productive to the unproductive season [70–75]. Measured BP rates determined for summer during this study are representative for the Fram Strait, i.e. surface BP $1.12 \pm 0.4\,\mu g\,C\,l^{-1}\,d^{-1}$ is very close to $1.14 \pm 0.4\,\mu g\,C\,l^{-1}\,d^{-1}$ observed between 0.8–9.5°E in 2011 [60]. The fourfold decline observed from summer to autumn is similar to the decreases previously reported for coastal regions such as Franklin Bay, Canada [70,72] and Kongsfjorden, Svalbard [71]. In addition to BP, the bacterial abundance and the proportion of HNA declined from summer to autumn. HNA are considered to represent the more metabolically active subpopulation that also appears to be substrate-driven [60,76]. Consequently, as semi-labile DOC components declined so did BP and the proportion of HNA, which suggests that bacteria are primarily controlled by the availability of semi-labile DOC in summer and autumn (figure 4). However, semi-labile DOC can be equally as important as temperature in controlling bacterial activity [10,45,77,78]. Our study does not directly support this since temperatures remained unchanged and BP still declined from summer to autumn, but synergistic combined effects could arise during other seasons or in the future due to warming. Synergistic effects have been observed if the demand for labile organic matter is met [10]. When future scenarios of climate warming are taken into account, an elevated release of semi-labile DOC in summer could lead to an increase of BP under warmer temperatures. The synergistic effects may be less pronounced in autumn and winter when bacteria consume organic matter with a more refractory state. Alternatively, a rise in temperature might also allow microbial degradation of refractory compounds [79], indicating that the reactivity of DOC could be less controlling for BP in the future. At the time of our study, the bioavailability of DOM has been the dominant control on bacterial activity during the productive and unproductive season. This, however, does not rule out the possibility of synergistic effects in the future.

Bacteria might further supplement their demand for labile components by accessing the dynamic continuum of gel particles. Precursors of gel particles like TEP are released by phytoplankton during the senescent bloom phase [21,80,81]. In particular, the inter-annual variability of TEP in the Fram Strait has been related to the abundance of the prymnesiophyte *Phaeocystis pouchetii* [80]. The twofold higher phytoplankton biomass and amounts of TEP in our study compared to previous observations by Busch *et al.* [82] suggests that the phytoplankton community release different concentrations of TEP into the water column during summer. To the best of our knowledge, our study is the first to show that TEP abundance, area and carbon content decreased more than twofold from summer to autumn (figures 2 and 4). The decrease in abundance and carbon content of TEP indicates that the particle content attributed to *P. pouchettii* diminishes quickly over time [83]. Within a given season, TEP could have been subject to microbial remineralization by extracellular enzymes [81,84], coagulation processes and sinking

into the deeper water column [82]. In contrast to TEP, CSP abundance and area declined by a factor less than one between the two seasons (figure 2, table 1). The production of CSP has been related to the picocyanobacterium *Synechococcus* spp. [85], which is highly abundant in the Arctic gateway throughout the year [86]. Again, amounts of CSP in summer and autumn were twice as high compared to 2015 [82], suggesting that formation by phytoplankton precursors, cell breakage and lysis [25] was higher during our study. Therefore, our results imply that cell deaths from the diatom-dominated summer bloom and the production by *Synechococcus* continue to release CSP until autumn. The continued amounts of CSP provide protein-rich micro gels for bacterial degradation after the dissolved pool of dHAA has been used. Our results show the loss of TEP and relative enrichment of CSP from summer to autumn thereby suggesting that gel particles could provide different temporal functions to the microbial food web. Future investigations of gel particle composition and the associated community composition might resolve whether the two types of particles provide different micro-niches for particle-attached bacteria at different times of the year [87–89].

Microbial dynamics within the Arctic ecosystem are seasonally and regionally variable, which makes an assessment of future changes challenging. Climate change associated alterations, such as rising temperatures and decreasing nutrient budgets, hold the potential to support phytoplankton release of semi-labile DOC that could support higher BP rates in summer and the beginning of autumn. Unfortunately, the lack of data for autumn 2018 did not allow us to discuss nutrients in the scope of this study. In the future, an increase in the amount of bioavailable DOM could stimulate the competition for mineral nutrients between phytoplankton and bacteria [90], releasing more CO_2 during bacterial respiration. Therefore, future changes to BP might reduce the net community production in the microbial food web and weaken CO_2 sequestration in the Arctic [27]. As such, parameters characterizing microbial food web dynamics, including components within semi-labile DOM, are of importance if we aim to assess future carbon cycling in the changing Arctic ecosystem.

5. Conclusion

Our observations demonstrate the importance of studying the effect of seasonal DOM dynamics on the microbial food web. Sampling in summer and autumn has allowed us to evaluate part of the seasonal shifts in microbial cycling of organic matter within the Fram Strait. Elevated concentrations of semi-labile DOC indicate an accumulation of recently produced DOM in summer. In autumn, the decrease in semi-labile DOC coincided with a decline in bacterial abundances and BP. Furthermore, we observed clear differences in the seasonal progression of gel particles with a twofold decrease in TEP and relative enrichment in CSP between summer and autumn. Our study highlighted that the availability of DOM shifts from summer to autumn and controls DOM–microbe interactions in the Fram Strait. Understanding the seasonal shifts in microbial cycling is of great importance in vulnerable environments like the Arctic, since seasonality may change in the future and potentially weaken the CO_2 sequestration in the Arctic Ocean.

Data accessibility. Data are available on PANGAEA Database [91,92].

Authors' contributions. A.v.J. and A.E. conceived the study, analysed and interpreted the data. A.v.J. and J.G. collected the samples and conducted the BP measurements. E.-M.N. provided chlorophyll data. All authors contributed to writing the manuscript.

Competing interests. We declare we have no competing interests.

Funding. The funding was provided by the Helmholtz Association and by the MicroARC project (grant no. 03F0802A) within the Changing Arctic Ocean program, jointly funded by the UKRI Natural Environment Research Council (NERC) and the German Federal Ministry of Education and Research (BMBF).

Acknowledgements. We thank the crew of the RV Polarstern and RV Maria S. Merian for their helpful support in obtaining the samples. A special thank you to Tania Klüver, Sandra Golde, Jon Roa, Sandra Murawski and Nadine Knüppel in helping with sampling on board or with analysis in the laboratory.

References

1. Masson-Delmotte V *et al.* 2018 Global warming of 1.5°C: an IPCC special report on the impacts of global warming of 1.5°C above pre-industrial levels and related global greenhouse gas emission pathways, in the context of strengthening the global response to the threat of climate change (eds V Masson-Delmotte, P Zhai, H-O Pörtner, D Roberts, J Skea, PR Shukla, A Pirani, W Moufouma-Okia, C Péan, R Pidcock, S Connors, JBR Matthews, Y Chen, X Zhou, MI Gomis, E Lonnoy, T Maycock, M Tignor, T Waterfield), pp. 1–28. See https://www.ipcc.ch/site/assets/uploads/sites/2/2019/06/SR15_Full_Report_Low_Res.pdf.
2. National Snow Snow Ice Data Center. Arctic sea ice at minimum extent for 2018, 2018. See https://nsidc.org/news/newsroom/arctic-sea-ice-2018-minimum-extent.
3. Comiso JC. 2012 Large decadal decline of the Arctic multiyear ice cover. *J. Clim.* **25**, 1176–1193. (doi:10.1175/JCLI-D-11-00113.1)
4. Kashiwase H, Ohshima KI, Nihashi S, Eicken H. 2017 Evidence for ice-ocean albedo feedback in the Arctic Ocean shifting to a seasonal ice zone. *Sci. Rep.* **7**, 8170. (doi:10.1038/s41598-017-08467-z)
5. Maslanik J, Stroeve J, Fowler C, Emery W. 2011 Distribution and trends in Arctic sea ice age through spring 2011. *Geophys. Res. Lett.* **38**, L13502. (doi:10.1029/2011GL047735)
6. Nghiem SV, Chao Y, Neumann G, Li P, Perovich DK, Street T, Clemente-Colón P. 2006 Depletion of perennial sea ice in the East Arctic Ocean. *Geophys. Res. Lett.* **33**, L17501. (doi:10.1029/2006GL027198)
7. Arrigo KR, van Dijken GL. 2015 Continued increases in Arctic Ocean primary production. *Prog. Oceanogr.* **136**, 60–70. (doi:10.1016/j.pocean.2015.05.002)
8. Kirchman DL, Morán XAG, Ducklow H. 2009 Microbial growth in the polar oceans—role of temperature and potential impact of climate change. *Nat. Rev. Microbiol.* **7**, 451–459. (doi:10.1038/nrmicro2115)
9. Ducklow HW, Schofield O, Vernet M, Stammerjohn S, Erickson M. 2012 Multiscale control of bacterial production by phytoplankton dynamics and sea ice along the western Antarctic Peninsula: a regional and decadal investigation. *J. Mar. Syst.* **98–99**, 26–39. (doi:10.1016/j.jmarsys.2012.03.003)
10. Piontek J, Sperling M, Nöthig EM, Engel A. 2015 Multiple environmental changes induce interactive effects on bacterial degradation activity in the Arctic Ocean. *Limnol. Oceanogr.* **60**, 1392–1410. (doi:10.1002/lno.10112)
11. Hansell DA, Carlson CA, Repeta DJ, Schlitzer R. 2009 Dissolved organic matter in the ocean: a controversy stimulates new insights. *Oceanography* **22**, 202–211. (doi:10.5670/oceanog.2009.109)
12. Skoog A, Benner R. 1997 Aldoses in various size fractions of marine organic matter: implications for carbon cycling. *Limnol. Oceanogr.* **42**, 1803–1813. (doi:10.4319/lo.1997.42.8.1803)
13. Goldberg SJ, Carlson CA, Hansell DA, Nelson NB, Siegel DA. 2009 Temporal dynamics of dissolved combined neutral sugars and the quality of dissolved organic matter in the Northwestern Sargasso Sea. *Deep Sea Res. Part I Oceanogr. Res. Pap.* **56**, 672–685. (doi:10.1016/j.dsr.2008.12.013)
14. Goldberg SJ, Carlson CA, Brzezinski M, Nelson NB, Siegel DA. 2011 Systematic removal of neutral sugars within dissolved organic matter across ocean basins. *Geophys. Res. Lett.* **38**, L17606. (doi:10.1029/2011GL048620)
15. Engel A, Harlay J, Piontek J, Chou L. 2012 Contribution of combined carbohydrates to dissolved and particulate organic carbon after the spring bloom in the northern Bay of Biscay (North-Eastern Atlantic Ocean). *Cont. Shelf Res.* **45**, 42–53. (doi:10.1016/j.csr.2012.05.016)
16. Meng S, Liu Y. 2016 New insights into transparent exopolymer particles (TEP) formation from precursor materials at various Na^+/Ca^{2+} ratios. *Sci. Rep.* **6**, 19747. (doi:10.1038/srep19747)
17. Verdugo P, Alldredge AL, Azam F, Kirchman DL, Passow U, Santschi PH. 2004 The oceanic gel phase: a bridge in the DOM–POM continuum. *Mar. Chem.* **92**, 67–85. (doi:10.1016/j.marchem.2004.06.017)
18. Logan BE, Grossart HP, Simon M. 1994 Direct observation of phytoplankton, TEP and aggregates on polycarbonate filters using brightfield microscopy. *J. Plankton Res.* **16**, 1811–1815. (doi:10.1093/plankt/16.12.1811)

19. Mari X, Kiørboe T. 1996 Abundance, size distribution and bacterial colonization of transparent exopolymeric particles (TEP) during spring in the Kattegat. *J. Plankton Res.* **18**, 969–986. (doi:10.1093/plankt/18.6.969)
20. Engel A, Goldthwait S, Passow U, Alldredge A. 2002 Temporal decoupling of carbon and nitrogen dynamics in a mesocosm diatom bloom. *Limnol. Oceanogr.* **47**, 753–761. (doi:10.4319/lo.2002.47.3.0753)
21. Passow U. 2002 Transparent exopolymer particles (TEP) in aquatic environments. *Prog. Oceanogr.* **55**, 287–333. (doi:10.1016/S0079-6611(02)00138-6)
22. Engel A. 2009 Determination of marine gel particles. In *Practical guidelines for the analysis of seawater* (ed O Wurl), pp. 125–143. Clermont, FL: CRC Press.
23. Long RA, Azam F. 1996 Abundant protein-containing particles in the sea. *Aquat. Microb. Ecol.* **10**, 213–221. (doi:10.3354/ame010213)
24. Thornton DCO. 2018 Coomassie stainable particles (CSP): protein containing exopolymer particles in the ocean. *Front. Mar. Sci.* **5**, 206. (doi:10.3389/fmars.2018.00206)
25. Verdugo P. 2012 Marine microgels. *Annu. Rev. Mar. Sci.* **4**, 375–400. (doi:10.1146/annurev-marine-120709-142759)
26. Bar-Zeev E, Berman-Frank I, Girshevitz O, Berman T. 2012 Revised paradigm of aquatic biofilm formation facilitated by microgel transparent exopolymer particles. *Proc. Natl Acad. Sci. USA* **109**, 9119–9124. (doi:10.1073/pnas.1203708109)
27. Vernet M, Ellingsen IH, Seuthe L, Slagstad D, Cape MR, Matrai PA. 2019 Influence of phytoplankton advection on the productivity along the Atlantic Water inflow to the Arctic Ocean. *Front. Mar. Sci.* **6**, 583. (doi:10.3389/fmars.2019.00583)
28. Forest A *et al.* 2011 Biogenic carbon flows through the planktonic food web of the Amundsen Gulf (Arctic Ocean): a synthesis of field measurements and inverse modeling analyses. *Prog. Oceanogr.* **91**, 410–436. (doi:10.1016/j.pocean.2011.05.002)
29. Maranger R, Vaqué D, Nguyen D, Hébert MP, Lara E. 2015 Pan-Arctic patterns of planktonic heterotrophic microbial abundance and processes: controlling factors and potential impacts of warming. *Prog. Oceanogr.* **139**, 221–232. (doi:10.1016/j.pocean.2015.07.006)
30. Evans CA, O'Reily JE, Thomas JP. 1987 *A handbook for measurement of chlorophyll a and primary production*. College Station, TX: Texas A & M University.
31. Engel A, Galgani L. 2016 The organic sea-surface microlayer in the upwelling region off the coast of Peru and potential implications for air-sea exchange processes. *Biogeosciences* **13**, 989–1007. (doi:10.5194/bg-13-989-2016)
32. Murphy J, Riley JP. 1962 A modified single solution method for the determination of phosphate in natural waters. *Anal. Chim. Acta* **27**, 31–36. (doi:10.1016/S0003-2670(00)88444-5)
33. Engel A, Händel N. 2011 A novel protocol for determining the concentration and composition of sugars in particulate and in high molecular weight dissolved organic matter (HMW-DOM) in seawater. *Mar. Chem.* **127**, 180–191. (doi:10.1016/j.marchem.2011.09.004)
34. Dittmar T, Cherrier J, Ludwichowski K-U. 2009 The analysis of amino acids in seawater. In *Practical guidelines for the analysis of seawater* (ed. O Wurl), pp. 67–77. Clermont, FL: CRC Press.
35. Lindroth P, Mopper K. 1979 High performance liquid chromatographic determination of subpicomole amounts of amino acids by precolumn fluorescence derivatization with o-phthaldialdehyde. *Anal. Chem.* **51**, 1667–1674. (doi:10.1021/ac50047a019)
36. Alldredge AL, Passow U, Logan BE. 1993 The abundance and significance of a class of large, transparent organic particles in the ocean. *Deep Sea Res. Part I Oceanogr. Res. Pap.* **40**, 1131–1140. (doi:10.1016/0967-0637(93)90129-Q)
37. Ling SC, Alldredge AL. 2003 Does the marine copepod Calanus pacificus consume transparent exopolymer particles (TEP)? *J. Plankton Res.* **25**, 507–515. (doi:10.1093/plankt/25.5.507)
38. Mari X, Burd A. 1998 Seasonal size spectra of transparent exopolymeric particles (TEP) in a coastal sea and comparison with those predicted using coagulation theory. *Mar. Ecol. Prog. Ser.* **163**, 63–76. (doi:10.3354/meps163063)
39. Mari X. 1999 Carbon content and C:N ratio of transparent exopolymeric particles (TEP) produced by bubbling exudates of diatoms. *Mar. Ecol. Progr. Ser.* **183**, 59–71. (doi:10.3354/meps183059)

40. Bouvier T, Del Giorgio PA, Gasol JM. 2007 A comparative study of the cytometric characteristics of High and Low nucleic-acid bacterioplankton cells from different aquatic ecosystems. *Environ. Microbiol.* **9**, 2050–2066. (doi:10.1111/j.1462-2920.2007.01321.x)
41. Robertson BR, Button DK. 1989 Characterizing aquatic bacteria according to population, cell size, and apparent DNA content by flow cytometry. *Cytometry* **10**, 70–76. (doi:10.1002/cyto.990100112)
42. Sherr EB, Sherr BF, Longnecker K. 2006 Distribution of bacterial abundance and cell-specific nucleic acid content in the Northeast Pacific Ocean. *Deep Sea Res. Part I Oceanogr. Res. Pap.* **53**, 713–725. (doi:10.1016/j.dsr.2006.02.001)
43. Smith DC, Azam F. 1992 A simple, economical method for measuring bacterial protein synthesis rates in seawater using 3H-leucine. *Mar. Microb. Food Webs* **6**, 107–114.
44. Simon M, Azam F. 1989 Protein content and protein synthesis rates of planktonic marine bacteria. *Mar. Ecol. Prog. Ser.* **51**, 201–213. (doi:10.3354/meps051201)
45. Kirchman DL, Malmstrom RR, Cottrell MT. 2005 Control of bacterial growth by temperature and organic matter in the Western Arctic. *Deep Sea Res. Part II Top. Stud. Oceanogr.* **52**, 3386–3395. (doi:10.1016/j.dsr2.2005.09.005)
46. Ihaka R, Gentleman R. 1996 R: a language for data analysis and graphics. *J. Comput. Graph. Stat.* **5**, 299.
47. Laird NM, Ware JH. 1982 Random-effect models for longitudinal data. *Biometrics* **38**, 963–974. (doi:10.2307/2529876)
48. Verbeke G, Molenberghs G. 2000 *Linear mixed models for longitudinal data*. Heidelberg, New York, NY: Springer.
49. Nakagawa S, Schielzeth H. 2013 A general and simple method for obtaining R^2 from generalized linear mixed-effects models. *Methods Ecol. Evol.* **4**, 133–142. (doi:10.1111/j.2041-210x.2012.00261.x)
50. Vihtakari M. PlotSvalbard: PlotSvalbard - Plot research data from Svalbard on maps. See https://github.com/MikkoVihtakari/PlotSvalbard.
51. Wickham H. 2016 tidyverse: Easily Install and Load 'Tidyverse' Packages. See https://cran.r-project.org/package=tidyverse.
52. Pinheiro J, Bates D, DebRoy S, Sarkar D, R Core Team. 2019 nlme: Linear and nonlinear mixed effects models. See https://cran.r-project.org/web/packages/nlme/index.html
53. Lefcheck JS. 2016 PIECEWISESEM: Piecewise structural equation modelling in R for ecology, evolution, and systematics. *Methods Ecol. Evol.* **7**, 573–579. (doi:10.1111/2041-210X.12512)
54. Hothorn T, Bretz F, Westfall P. 2008 Simultaneous inference in general parametric models. *Biom. J.* **50**, 346–363. (doi:10.1002/bimj.200810425)
55. Lenth RV. 2016 Least-squares means: the R package lsmeans. *J. Stat. Softw.* **69**, 1–33. (doi:10.18637/jss.v069.i01)
56. Fox J, Weisberg S. 2019 An R companion to applied regression. Thousand Oaks, CA: Sage.
57. Husson F, Josse J, Le S, Mazet J. Multivariate exploratory data analysis and data mining. *J. Stat. Softw.* **25**, 1–19.
58. Wright K. 2018 corrgram: plot a correlogram, R package version 1.13. See https://cran.r-project.org/package=corrgram.
59. Kaiser K, Benner R. 2009 Biochemical composition and size distribution of organic matter at the Pacific and Atlantic time-series stations. *Mar. Chem.* **113**, 63–77. (doi:10.1016/j.marchem.2008.12.004)
60. Piontek J, Sperling M, Nöthig E-M, Engel A. 2014 Regulation of bacterioplankton activity in Fram Strait (Arctic Ocean) during early summer: the role of organic matter supply and temperature. *J. Mar. Syst.* **132**, 83–94. (doi:10.1016/j.jmarsys.2014.01.003)
61. Ittekkot V, Brockmann U, Michaelis W, Degens ET. 1981 Dissolved free and combined carbohydrates during a phytoplankton bloom in the northern North Sea. *Mar. Ecol. Prog. Ser.* **4**, 299–305. (doi:10.3354/meps004299)
62. Panagiotopoulos C, Sempéré R, Jacq V, Charrière B. 2014 Composition and distribution of dissolved carbohydrates in the Beaufort Sea Mackenzie margin (Arctic Ocean). *Mar. Chem.* **166**, 92–102. (doi:10.1016/j.marchem.2014.09.004)
63. Amon RMW, Fitznar HP, Benner R. 2001 Linkages among the bioreactivity, chemical composition, and diagenetic state of marine dissolved organic matter. *Limnol. Oceanogr.* **46**, 287–297. (doi:10.4319/lo.2001.46.2.0287)

64. Davis J, Benner R. 2005 Seasonal trends in the abundance, composition and bioavailability of particulate and dissolved organic matter in the Chukchi/Beaufort Seas and western Canada Basin. *Deep Sea Res. Part II Top. Stud. Oceanogr.* **52**, 3396–3410. (doi:10.1016/j.dsr2.2005.09.006)
65. Davis J, Benner R. 2007 Quantitative estimates of labile and semi-labile dissolved organic carbon in the western Arctic Ocean: a molecular approach. *Limnol. Oceanogr.* **52**, 2434–2444. (doi:10.4319/lo.2007.52.6.2434)
66. Meon B, Amon RMW. 2004 Heterotrophic bacterial activity and fluxes of dissolved free amino acids and glucose in the Arctic rivers Ob, Yenisei and the adjacent Kara Sea. *Aquat. Microb. Ecol.* **37**, 121–135. (doi:10.3354/ame037121)
67. Rich J, Gosselin M, Sherr E, Sherr B, Kirchman DL. 1997 High bacterial production, uptake and concentrations of dissolved organic matter in the Central Arctic Ocean. *Deep Sea Res. Part II Top. Stud. Oceanogr.* **44**, 1645–1663. (doi:10.1016/S0967-0645(97)00058-1)
68. Shen Y, Fichot CG, Benner R. 2012 Dissolved organic matter composition and bioavailability reflect ecosystem productivity in the Western Arctic Ocean. *Biogeosciences* **9**, 4993–5003. (doi:10.5194/bg-9-4993-2012)
69. Shen Y, Benner R, Kaiser K, Fichot CG, Whitledge TE. 2018 Pan-arctic distribution of bioavailable dissolved organic matter and linkages with productivity in ocean margins. *Geophys. Res. Lett.* **45**, 1490–1498. (doi:10.1002/2017GL076647)
70. Garneau MÈ, Roy S, Lovejoy C, Gratton Y, Vincent WF. 2008 Seasonal dynamics of bacterial biomass and production in a coastal arctic ecosystem: Franklin Bay, western Canadian Arctic. *J. Geophys. Res. Oceans* **113**, 1–15. (doi:10.1029/2007JC004281)
71. Iversen KR, Seuthe L. 2011 Seasonal microbial processes in a high-latitude fjord (Kongsfjorden, Svalbard): I. Heterotrophic bacteria, picoplankton and nanoflagellates. *Polar Biol.* **34**, 731–749. (doi:10.1007/s00300-010-0929-2)
72. Nguyen D, Maranger R, Tremblay JÈ, Gosselin M. 2012 Respiration and bacterial carbon dynamics in the Amundsen Gulf, western Canadian Arctic. *J. Geophys. Res. Oceans* **117**, C00G16. (doi:10.1029/2011JC007343)
73. Sherr BF, Sherr EB. 2003 Community respiration/production and bacterial activity in the upper water column of the central Arctic Ocean. *Deep Sea Res. Part I Oceanogr. Res. Pap.* **50**, 529–542. (doi:10.1016/S0967-0637(03)00030-X)
74. Sherr EB, Sherr BF, Wheeler PA, Thompson K. 2003 Temporal and spatial variation in stocks of autotrophic and heterotrophic microbes in the upper water column of the central Arctic Ocean. *Deep Sea Res. Part I Oceanogr. Res. Pap.* **50**, 557–571. (doi:10.1016/S0967-0637(03)00031-1)
75. Vaqué D, Guadayol Ò, Peters F, Felipe J, Angel-Ripoll L, Terrado R, Lovejoy C, Pedrós-Alió C. 2008 Seasonal changes in planktonic bacterivory rates under the ice-covered coastal Arctic Ocean. *Limnol. Oceanogr.* **53**, 2427–2438. (doi:10.4319/lo.2008.53.6.2427)
76. Cuevas LA, Egge JK, Thingstad TF, Töpper B. 2011 Organic carbon and mineral nutrient limitation of oxygen consumption, bacterial growth and efficiency in the Norwegian Sea. *Polar Biol.* **34**, 871–882. (doi:10.1007/s00300-010-0944-3)
77. Kirchman DL, Hill V, Cottrell MT, Gradinger R, Malmstrom RR, Parker A. 2009 Standing stocks, production, and respiration of phytoplankton and heterotrophic bacteria in the western Arctic Ocean. *Deep Sea Res. Part II Top. Stud. Oceanogr.* **56**, 1237–1248. (doi:10.1016/j.dsr2.2008.10.018)
78. Sala MM, Terrado R, Lovejoy C, Unrein F, Pedrós-Alió C. 2008 Metabolic diversity of heterotrophic bacterioplankton over winter and spring in the coastal Arctic Ocean. *Environ. Microbiol.* **10**, 942–949. (doi:10.1111/j.1462-2920.2007.01513.x)
79. Lønborg C, Álvarez-Salgado XA, Letscher RT, Hansell DA. 2018 Large stimulation of recalcitrant dissolved organic carbon degradation by increasing ocean temperatures. *Front. Mar. Sci.* **4**, 436. (doi:10.3389/fmars.2017.00436)
80. Engel A, Piontek J, Metfies K, Endres S, Sprong P, Peeken I, Gäbler-Schwarz S, Nöthig EM. 2017 Inter-annual variability of transparent exopolymer particles in the Arctic Ocean reveals high sensitivity to ecosystem changes. *Sci. Rep.* **7**, 4129. (doi:10.1038/s41598-017-04106-9)
81. Ortega-Retuerta E, Marrasé C, Muñoz-Fernández A, Sala MM, Simó R, Gasol JM. 2018 Seasonal dynamics of transparent exopolymer particles (TEP) and their drivers in the coastal NW Mediterranean Sea. *Sci. Total Environ.* **631–632**, 180–190. (doi:10.1016/j.scitotenv.2018.02.341)

82. Busch K, Endres S, Iversen MH, Michels J, Nöthig EM, Engel A. 2017 Bacterial colonization and vertical distribution of marine gel particles (TEP and CSP) in the Arctic Fram Strait. *Front. Mar. Sci.* **4**, 1–14. (doi:10.3389/fmars.2017.00166)
83. Reigstad M, Wassmann P. 2007 Does *Phaeocystis* spp. contribute significantly to vertical export of organic carbon? *Biogeochemistry* **83**, 217–234. (doi:10.1007/s10533-007-9093-3)
84. Berman-Frank I, Spungin D, Rahav E, Van Wambeke F, Turk-Kubo K, Moutin T. 2016 Dynamics of transparent exopolymer particles (TEP) during the VAHINE mesocosm experiment in the New Caledonian lagoon. *Biogeosciences* **13**, 3793–3805. (doi:10.5194/bg-13-3793-2016)
85. Cisternas-Novoa C, Lee C, Engel A. 2015 Transparent exopolymer particles (TEP) and Coomassie stainable particles (CSP): differences between their origin and vertical distributions in the ocean. *Mar. Chem.* **175**, 56–71. (doi:10.1016/j.marchem.2015.03.009)
86. Paulsen ML, Doré H, Garczarek L, Seuthe L, Müller O, Sandaa R-A, Bratbak G, Larsen A. 2016 *Synechococcus* in the Atlantic gateway to the Arctic Ocean. *Front. Mar. Sci.* **3**, 191. (doi:10.3389/fmars.2016.00191)
87. Carrias JF, Serre JP, Sime-Ngando T, Amblard C. 2002 Distribution, size, and bacterial colonization of pico- and nano-detrital organic particles (DOP) in two lakes of different trophic status. *Limnol. Oceanogr.* **47**, 1202–1209. (doi:10.4319/lo.2002.47.4.1202)
88. Fadeev E, Salter I, Schourup-Kristensen V, Nöthig E-M, Metfies K, Engel A, Piontek J, Boetius A, Bienhold C. 2018 Microbial communities in the east and west Fram Strait during sea ice melting season. *Front. Mar. Sci.* **5**, 429. (doi:10.3389/fmars.2018.00429)
89. Zäncker B, Engel A, Cunliffe M. 2019 Bacterial communities associated with individual transparent exopolymer particles (TEP). *J. Plankton Res.* **41**, 561–565. (doi:10.1093/plankt/fbz022)
90. Thingstad TF *et al.* 2008 Counterintuitive carbon-to-nutrient coupling in an Arctic pelagic ecosystem. *Nature* **455**, 387–390. (doi:10.1038/nature07235)
91. von Jackowski A, Engel A. 2019 Physical oceanography measured on water bottle samples during Maria S. Merian cruise MSM77. Technical report. See https://doi.pangaea.de/10.1594/PANGAEA.907467.
92. von Jackowski A, Grosse J, Nöthig E-M, Engel A. 2020 Bacterial production and organic matter of POLARSTERN cruise PS114 and Maria S. Merian cruise MSM77. See https://doi.pangaea.de/10.1594/PANGAEA.915751.